Redox Biology 83 (2025) 103615

Contents lists available at ScienceDirect

Redox Biology

journal homepage: www.elsevier.com/locate/redox

GPX4 deficiency-induced ferroptosis drives endometrial epithelial fibrosis in polycystic ovary syndrome

Zhenhong Ye [a,b,c,d,1], Ming Cheng [a,b,c,d,1], Weisi Lian [a,b,c,d,1], Yueqi Leng [a,b,c,d], Xunsi Qin [a,b,c,d], Yue Wang [a,b,c,d], Ping Zhou [a,b,c,d], Xiyao Liu [a,b,c,d], Tianliu Peng [a,b,c,d], Ruiqi Wang [a,b,c,d], Yilei He [a,b,c,d], Heng Pan [a,b,c,d,***], Yue Zhao [a,b,c,d,**], Rong Li [a,b,c,d,*]

[a] State Key Laboratory of Female Fertility Promotion, Center for Reproductive Medicine, Department of Obstetrics and Gynecology, Peking University Third Hospital, Beijing, China
[b] National Clinical Research Center for Obstetrics and Gynecology, Peking University Third Hospital, Beijing, China
[c] Key Laboratory of Assisted Reproduction, Ministry of Education, Beijing, China
[d] Beijing Key Laboratory of Reproductive Endocrinology and Assisted Reproductive Technology, Beijing, China

ARTICLE INFO

Keywords:
Polycystic ovary syndrome
Ferroptosis
Endometrial fibrosis
Organoid
Female infertility

ABSTRACT

The increased risk of infertility and endometrial lesions (such as endometrial hyperplasia or cancer) in polycystic ovary syndrome (PCOS) are closely associated with the lack of cyclical transformation in the endometrium. However, the underlying mechanisms remain incompletely understood. Though integrating single-cell RNA-sequencing, transcriptomics, and metabolomics analysis, we found that glutathione (GSH) metabolism disorder and the overactivation of ferroptosis, triggered by glutathione peroxidase 4 (GPX4) deficiency in endometrial epithelial cells, were the consequences of the prolonged endometrial proliferative phase in PCOS. This change may collectively contribute to some extent to decidualization failure. We further performed GSVA analysis and determined that the negative correlation between ferroptosis and fibrosis-related pathway was the most significant. Therefore, we first confirmed the presence of fibrosis in the proliferative endometrium of PCOS and PCOS-like mouse uteri. Additionally, by establishing endometrial organoids (EEOs) models and in vitro cell line models, we demonstrated that GPX4 deficiency contributed to extracellular matrix remodeling and excessive collagen deposition, via activating the TGF-β1/Smad2/3 pathway, which ultimately accelerated fibrosis. GSH intervention to the EEOs of PCOS could alleviate their fibrotic phenotypes at different stages. These findings may serve as a promising therapeutic target for PCOS-related endometrial dysfunction, as well as valuable strategies for improving PCOS-related adverse pregnancy outcomes.

1. Introduction

Polycystic ovary syndrome (PCOS) is a complex reproductive endocrine and metabolic disorder. The prevalence of PCOS in Chinese women reached in 7.8 %, nearly 65 % higher than a decade ago, affecting the health of women in the reproductive age [1]. The main clinical manifestations were hyperandrogenemia, oligomenorrhea or amenorrhea and polycystic ovary [2]. In addition to reproductive disturbances, PCOS patients also have metabolic abnormalities, including obesity, dyslipidemia, insulin resistance, metabolic syndrome, and chronic low-grade

* Corresponding author. Department of Obstetrics and Gynecology, Peking University Third Hospital, No.49 North HuaYuan Road, HaiDian District, Beijing, 100191, China.
** Corresponding author. Department of Obstetrics and Gynecology, Peking University Third Hospital, No.49 North HuaYuan Road, HaiDian District, Beijing, 100191, China.
*** Corresponding author. Department of Obstetrics and Gynecology, Peking University Third Hospital, No.49 North HuaYuan Road, HaiDian District, Beijing, 100191, China.
E-mail addresses: hep2007@bjmu.edu.cn (H. Pan), zhaoyue0630@163.com (Y. Zhao), roseli001@sina.com (R. Li).
[1] These authors contributed equally to this study.

https://doi.org/10.1016/j.redox.2025.103615
Received 4 February 2025; Received in revised form 19 March 2025; Accepted 24 March 2025
Available online 25 March 2025

inflammation [3]. Previous studies have shown that PCOS have an increased risk of adverse pregnancy outcomes, manifested as increased rates of spontaneous abortion and implantation failure, and decreased rates of live birth and clinical pregnancy [4]. After adjusting for various confounding factors, such as maternal age, body mass index (BMI), number of transplanted embryos, and embryo quality, the miscarriage rate and very preterm delivery remained higher in the PCOS [5]. Therefore, endometrial dysfunction may be one of the potential causes of adverse pregnancy outcomes in PCOS.

Under physiological conditions, the endometrium undergoes cyclical changes that are divided into the proliferative phase, secretory phase, and menstrual phase by the sequential action of estrogen and progesterone. Cell proliferation and mitotic activity, driven by high levels of estrogen, are strengthened during the proliferation phase. Subsequently, progesterone secreted by the corpus luteum after ovulation reduces cell proliferation, initiates the decidualization of stromal cells, and triggers the transition to the secretory phase [6]. The transformation of the endometrium from the proliferative to the secretory phase is a primary condition for embryo implantation [7]. PCOS patients have prolonged proliferation period due to long-term stimulation of estrogen, resulting in a significant increase in the risk of poor endometrial receptivity, endometrial atypical hyperplasia, and even the development of endometrial cancer [8]. However, the crucial molecular and corresponding mechanism of periodic transformation deficiency in PCOS endometrium remains poorly understood.

Recent studies have demonstrated that ferroptosis was involved in ovarian hormone synthesis and the endometrium response to hormones though modulating oxidative stress in ovarian granulosa cells [9], remodeling of uterine epithelial cells [10] and the proliferation of ectopic endometrium [11]. A meta-analysis showed that compared to the non-PCOS group, PCOS patients matched for age and BMI had significantly reduced levels of circulating glutathione (GSH) and increased levels of lipid peroxide malondialdehyde (MDA) [12]. This peroxidation environment created conditions for ferroptosis in PCOS endometrium. Ferroptosis was an iron-dependent cell death characterized by intracellular accumulation of iron and reactive oxygen species (ROS) leading to lipid peroxidation [13]. The antioxidant system played a key role in regulating ferroptosis. It mainly composed of glutathione peroxidase 4 (GPX4), guanosine triphosphate cyclase 1 (GCH1), dihydroorotate dehydrogenase (DHODH), ferroptosis inhibitory protein 1 (FSP1), etc. Among them, GPX4 was the exclusive enzyme in mammalian cells that could directly hydrolyze and clear lipid peroxides [14]. In this process, GSH acted as a cofactor of GPX4, transformed into oxidized glutathione (GSSG). The ratio of GSH/GSSG reflected the state of ferroptosis [15]. However, there is no metabolomics research applied to analyze the pathological changes of the PCOS endometrium. Besides, whether ferroptosis participated in the cyclical transformation disorder of the PCOS endometrium and the corresponding metabolic regulation mechanisms have not been elucidated, and further studies were needed.

Here, we used multi-omics data analysis including single-cell RNA sequencing (scRNA-seq), transcriptomics, and metabolomics to identify key biological events that mediate endometrial receptivity abnormalities in PCOS, namely, abnormal GSH metabolism and GPX4 deficiency-mediated ferroptosis activation. Clinical samples and animal models were used to characterize the presence of endometrial fibrosis in PCOS. Cell lines and organoid models were used to elucidate the molecular mechanism of fibrosis induced by ferroptosis, manifested as defective GPX4 expression in PCOS proliferative endometrial epithelial cells. Our study attempts to provide new targets for improving endometrial function and pregnancy outcomes in PCOS.

2. Materials and methods

2.1. Study population

This study has been approved by the Ethics Committee of Peking University Third Hospital (No. 2021-458-01) and has obtained informed consent from all participants.

We recruited Chinese women with 20 PCOS and 30 non-PCOS patients visited in the Reproductive Medicine Center of Peking University Third Hospital from January 2022 to December 2024. PCOS was diagnosed according to the Rotterdam criteria, which requires two or more of the following features: (1) oligoovulation and/or anovulation; (2) hyperandrogenism (clinical and/or biochemical traits); (3) polycystic ovaries. The exclusion criteria were the presence of pregnancy, metabolic or endocrine related disturbance (congenital adrenal hyperplasia, androgen-secreting tumors, hypogonadotropic hypogonadism, thyroid dysfunction, Cushing syndrome, hyperprolactinemia and premature ovarian failure), ovarian cysts or tumors, and chromosomal abnormalities. The non-PCOS patients included women attending the clinic owing to male azoospermia or tubal occlusion. The non-PCOS patients were required to have normal hormone levels, regular menstrual cycles, and normal ovarian morphology under ultrasound examination. All selected subjects were 20–38 years and have no history of taking hormones, insulin sensitizers, or lipid-lowering drugs within the past 3 months. Hysteroscopy was used to exclude intrauterine lesions. All selected patients underwent hysteroscopic examination during the proliferative phase and secretory phase. Endometrial tissue was obtained by hysteroscopic surgery from the surplus tissue sent for pathological examination.

2.2. Organoids isolation, culture and passaging

Endometrial epithelial cells were isolated from endometrial tissue by digestion with collagenase IV (Sigma-Aldrich, USA) for 15 min at 37 °C. If large cell clumps were observed, an additional 5-10 min of digestion was performed until most clumps became single cells. Digestion was terminated by adding an equal volume of advanced DMEM/F-12 (Gibco, USA). The cell suspension was filtered through 100 μm (Falcon, USA) and 40 μm (Falcon, USA) cell strainers, then centrifuged at 300 g for 5 min to retain glandular elements. The endometrial stromal cells (ESCs) were then resuspended in Dulbecco's modified eagle medium (DMEM)/F12 medium (without phenol red, Gibco) supplemented with 10 % fetal bovine serum (Charcoal/Dextran Stripped, CS-FBS, Gemini, USA) and plated in 12-cell plates. Cells in Matrigel (Corning, USA) were seeded in 24-cell plates and cultured in the expansion medium (ExM), contained with 1 % N2 (ThermoFisher, USA), 1 % B27 (ThermoFisher, USA), 1 % Glutamax (Gibco, USA), R-Spondin 1 (Novoprotein, China), Noggin (Novoprotein, China), 1.25 mM N-Acetylcysteine (Sigma-Aldrich, USA), 10 mM Nicotinamide (Sigma-Aldrich, USA), HGF (Novoprotein, China), EGF (Novoprotein, China), FGF10 (Novoprotein, China), 10 μM Y-27632 (MCE, USA), A83-01 (MCE, USA), ITS (ThermoFisher, USA) and Penicillin/Streptomycin solution (Gibco, USA). Medium was replaced every 2-3 days. Endometrial Organoids were passaged at a 1:2–1:3 ratio every 7-10 days for over 10 passages. For freezing, the medium was replaced with 1 mL TrypLETM Select (Gibco, USA) and organoids were incubated in TrypLE at 37 °C, triturated every 5 min until dissociated to single cells. Cells were then centrifuged at 300 g for 5 min, and the supernatant was removed. The cells were shock-frozen in liquid nitrogen.

2.3. Hormone treatment and differentiation of endometrial epithelial organoids (EEOs)

Hormonal stimulation assays were performed according to a previously published protocol with minor modifications. Briefly, EEOs were passaged routinely, and after 4 days of growth in ExM, they were primed with 10 nM β-estradiol (E2, Sigma-Aldrich, USA). After 48 h, the medium was replaced with the following conditions: i) untreated (ExM), ii) 10 nM E2, or iii) 10 nM E2 + 1 μM medroxyprogesterone acetate (MPA, MCE, USA) + 1 μM 8-Bromoadenosine 3',5'-cyclic monophosphate sodium salt (cAMP, Sigma, USA). Meanwhile, EEOs were treated with either GSH (Selleck, USA) or FIN56 (Selleck, USA). After 6 days, the

organoids were collected and used for subsequent experiments. For organoid differentiation, they were passaged routinely, and after 4 days in ExM, the medium was switched to differentiation medium (DM), which is ExM containing 10 nM E2 + 1 μM MPA + 1 μM cAMP. DM was supplemented with a combination of 1 μg/mL hCG (human Chorionic gonadotropin, Source Bioscience, USA), 20 ng/mL hPL (Human placental lactogen, R&D, USA) and 20 ng/mL PRL (Prolactin, Peprotech, USA) for another 10 days. After 6 days, the organoids were collected and used for subsequent experiments.

2.4. RNA isolation and RNA-seq analysis

According to the manufacturer's protocol, total RNA was extracted from proliferative endometrial tissue using TRIzol reagent (Invitrogen, USA). A total of 50 endometrial samples were subjected to RNA sequencing, including 30 non-PCOS and 20 PCOS patients. The clinical and biochemical characteristics of the two groups were shown in Supplementary Table 1. Used DESeq2 (v. 1.40.2 R package) for estimating variance-mean dependence in count data and testing differential gene expression based on a robust statistical framework using the negative binomial distribution. Transformed raw counts into Fragments Per Kilobase of transcript per Million mapped reads (FPKM) values for comparing gene expression levels across samples. The criteria for differentially expressed genes (DEGs) was determined by the p value $<$ 0.05 and the absolute value of fold change (FC) $>$ 1.5. The subsequent enrichment analysis was conducted using KEGG, and GSEA to explain the biological significance of DEGs in the context of cellular processes, molecular functions, and pathway involvement. All analysis were implemented in R environment v. 4.3.1.

2.5. Single-cell RNA-sequencing (scRNA-seq) data acquisition and analysis

We obtained scRNA-seq datasets of healthy patient endometrium during different menstrual cycles from the Gene Expression Omnibus (GEO) database (GSE111976). This dataset was generated using 10 × Genomics techniques and sequenced in paired-end reads on Nextseq (Illumina) platform including 10 women aged 18-34. Our single-cell analysis mainly focused on endometrial epithelial cells in the proliferative and secretory phases. To identify ferroptosis-related subpopulations, we used the AUCell package [16] to enrich activity scores of ferroptosis pathways within endometrial subpopulations. The FindAllMarkers function of the Seurat package was used to calculate DEGs between various cell types in the proliferative and secretory phases of endometrium, with a selection criterion of absolute $\log_2$FC $>$ 0.25 and p value $<$ 0.05.

2.6. Untargeted and targeted metabolomics sequencing and analysis

Endometrium tissue samples (15 non-PCOS and 15 PCOS patients) were analyzed by Waters ultrahigh performance liquid chromatography (UHPLC)-AB Sciex 5600 Q TOF mass spectrometer. The specific detection and metabolite annotation methods were described in the supplementary methods. Statistical analyses were performed using Metaboanalyst 5.0. After preprocessing the data with total sum-normalization and pareto-scaling, multidimensional statistical analyses were conducted.

The targeted metabolic profiling of endometrium tissue (35 non-PCOS and 35 PCOS patients) extracts was performed and analyzed by Metabo-Profile (Shanghai, China) as described in previous study [17]. Simply, an ultra-performance liquid chromatography coupled to tandem mass spectrometry (UPLC-MS/MS) system (ACQUITY UPLC-Xevo TQ-S, Waters Corp., Milford, MA, USA) was used to quantitate all targeted metabolites in this project. The raw data files generated by UPLC-MS/MS were processed using the TMBQ software (v1.0, Metabo-Profile, Shanghai, China) to perform peak integration, calibration, and quantitation for each metabolite.

The variable importance in the projection (VIP) value of each variable in the OPLS-DA model was calculated to assess its contribution to the classification. Student's t-test was performed to determine the significance of differences between two independent sample groups. VIP $>$1 and p value $<$ 0.05 were used to screen for significantly changed metabolites. The clinical and biochemical characteristics of the two groups were shown in Supplementary Table 2.

2.7. Quantitative reverse transcription polymerase chain reaction analysis (qPCR)

Total RNA was extracted from endometrial epithelium cells with TRIzol reagent (Invitrogen, USA), and cDNA was synthesized with the ReverTra Ace qPCR RT Kit (Toyobo, Japan). Quantitative PCR was performed using the SYBR Green PCR master mix (Invitrogen, USA), according to manufacturer's protocol in the ABI 7500 real-time PCR system (Applied Biosystems Inc). The primer sequences of the genes tested were shown in Supplementary Table 3.

2.8. Western blotting

Total protein extracted from endometrial epithelium cells were lysed in RIPA lysis buffer containing protease inhibitors and phosphatase inhibitors and quantified by a BCA assay (BCA Protein Assay Kit; Thermo Scientific, USA). The primary antibodies were applied according to the provided recommendations: anti-GPX4 (Abcam, Cat# ab125066), anti-SMAD2/3 (Cell Signaling Technology, Cat# 8685), anti-Phospho-SMAD2 (Ser465/467)/SMAD3(Ser423/425) (Cell Signaling Technology, Cat# 8828), anti-Fibronectin (Abcam, Cat# ab2413), and anti-VINCULIN antibody (Abcam, Cat# ab129002).

2.9. Histology and immunohistochemistry

The endometrial tissue from humans and mice were fixed with 4 % paraformaldehyde (PFA) and embed in paraffin. Immunohistochemistry was performed as described previously [18]. The primary antibodies included anti-GPX4 (Abcam, Cat# ab125066) and anti-4-HNE (Abcam, Cat# ab48506). Masson's Trichrome staining according to kit instruction (Solarbio, China). Scanned and recorded all slices using the NanoZoomer Digital Pathology slice scanner. Calculated the proportion of blue color in Masson trichrome staining using Image J software.

2.10. Immunofluorescence (IF)

Harvested organoids and performed immunofluorescence staining using the method described previously [19]. Briefly, the organoids were fixed with 1 mL 4 % PFA for 1 h at room temperature. Carefully removed PFA and permeate with 0.5 % Triton X-100/PBS for 10 min and then blocked with 3 % bovine serum albumin in PBS for 30 min. The organoids were incubated overnight with primary antibody and corresponding secondary antibodies conjugated with Alexa 488 or Alexa 555. Nuclear staining was carried out using DAPI (Solarbio, China). Obtained confocal images using a confocal microscope (Zeiss LSM980). The primary antibodies included anti-GPX4 (Abcam, Cat# ab125066), anti-SMAD2/3 (Cell Signaling Technology, Cat# 8685), anti-Phospho-SMAD2 (Ser465/467)/SMAD3(Ser423/425) (Cell Signaling Technology, Cat# 8828) and anti-Fibronectin (Abcam, Cat# ab2413).

2.11. Cell culture

The human endometrial epithelial cell line ishikawa was purchased by Pricella (Biotechnology Co., Ltd. China). Ishikawa cells were cultured in DMEM/F12 medium containing 10 % fetal bovine serum and 1 % penicillin streptomycin supplement, under a humidified atmosphere of

37 °C and 5 % CO_2. Using dimethyl sulfoxide (DMSO) as a control, ishikawa cells were treated with dihydrotestosterone (DHT) (GlpBio, USA), TGF-β1 (PeproTech, USA) or FIN56 (Selleck, USA) for subsequent experiments and detection.

2.12. siRNA silencing

Ishikawa cells were transfected with siRNA against *GPX4*: 1# 5′-GCTACAACGTCAAATTCGA-3′, 2# 5′-GTAACGAAGAGATCAAAGA-3′, 3# 5′-GAGGCAAGACCGAAGTAAA-3′ (RIBOBIO, China) with Opti-MEM

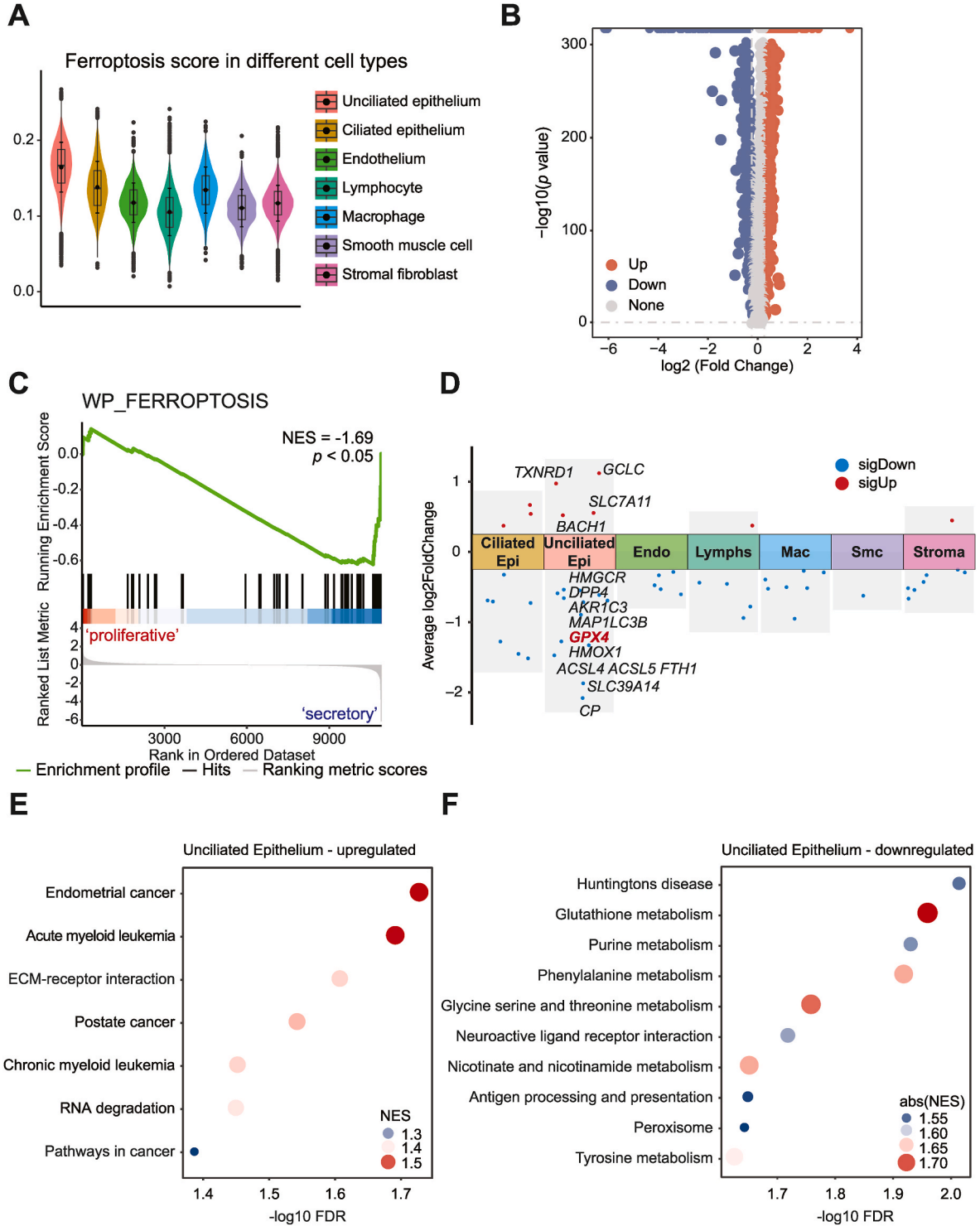

Fig. 1. Ferroptosis participated the periodic transformation of the normal endometrium during menstrual cycles. (**A**) Activation of seven cell types along the ferroptosis pathway. (**B**) Volcano plot illustrated differentially expressed genes between proliferative and secretory unciliated epithelium. Up-regulated genes were shown in red ($p < 0.05$); down-regulated genes were marked in blue ($p < 0.05$); non-significant genes were indicated in gray ($p > 0.05$). (**C**) GSEA analysis showed the differences in ferroptosis pathway between proliferative and secretory unciliated epithelium based on the WP database. (**D**) Volcano plot illustrated differentially expressed genes between the proliferative and secretory endometrium in each cell type. Up-regulated genes were shown in red ($p < 0.05$); down-regulated genes were marked in blue ($p < 0.05$). (**E** and **F**) KEGG pathway enrichment analysis of up-regulated (E) and down-regulated differential genes (**F**) in unciliated epithelium.

(Life Technologies Inc.) using lipofectamine™ RNAiMAX transfection reagent (Thermo Fisher Scientific, USA), according to the recommended protocol.

2.13. Statistical analysis

Data are expressed as the mean ± standard error of the mean (SEM) or standard deviation (SD), as stated in the figure legends. SPSS 26.0 and GraphPad Prism version 9.0 were used for statistical analysis. The sample distribution was determined by the Kolmogorov–Smirnov normality test. Statistical comparisons of patients with PCOS and the non-PCOS were made using Student's *t*-test or nonparametric test when appropriate. Statistically, a p value < 0.05 was considered a significant difference.

3. Results

3.1. Ferroptosis was involved in regulating the periodic transformation of physiological endometrial epithelial cells

To determine whether ferroptosis was involved in the cyclical transformation of the endometrium, we analyzed scRNA-seq data from GSE111976 dataset across the natural human menstrual cycle [20]. Based on cell specific marker genes (Fig. S1A), seven cell types were identified including unciliated epithelium, ciliated epithelium, endothelium, lymphocyte, macrophage, smooth muscle cell and stromal fibroblast (Fig. S1B). To confirm which cell type was most associated with ferroptosis, we calculated the ferroptosis pathway activity using the AUCell package in reference to the "WP_FERROPTOSIS" gene set in each cell type. As shown in Fig. 1A, unciliated epithelium was the highest ferroptosis activity. To further explore the key biological events involved in the transition of unciliated epithelium from the proliferative to the secretory phase, we conducted differential gene expression analysis between the two periods (Fig. 1B). Compared to the proliferative phase, the ferroptosis pathway was significantly enriched in secretory unciliated epithelium, as analyzed by gene set enrichment analysis (GSEA) (Fig. 1C). The volcano plot displayed ferroptosis-related differential genes between the two phases in epithelial cells and other cell types (Fig. 1D). Furthermore, Kyoto encyclopedia of genes and genomes (KEGG) analysis showed that downregulation of other signaling pathways related to endometrial function, such as endometrial cancer, extracellular matrix (ECM)-receptor interactions, RNA degradation, etc. (Fig. 1E). GSH metabolism, an upstream pathway closely associated with ferroptosis, was also significantly down-regulated (Fig. 1F). Therefore, it is crucial to reduce ferroptosis activity and GSH metabolism during the transformation of the unciliated epithelium to the secretory phase.

3.2. Transcriptomics of proliferative endometrium in PCOS revealed abnormal ferroptosis activity and GSH metabolism

To comprehensively investigate the differences in gene expression of proliferative endometrium between PCOS and non-PCOS patients, transcriptomics sequencing was performed. A total of 609 up-regulated and 1225 down-regulated genes were determined in the PCOS patients versus to the non-PCOS patients (Fig. 2A). KEGG enrichment analysis revealed that multiple biological processes, involving ECM-receptor interaction, focal adhesion, and cell adhesion molecules pathways, were significantly upregulated (Fig. 2B). Ferroptosis and GSH metabolism pathways were significantly downregulated (Fig. 2C), which were also observed in scRNA-seq enrichment analysis. To further clarify the reasons for the lack of periodicity in the PCOS endometrium, we intersected the differentially expressed genes enriched in ferroptosis and GSH metabolism from our transcriptomics and scRNA-seq data to identify key genes. We found that *GPX4* was the unique gene in both datasets (Fig. 2D). Its expression was significantly higher in secretory endometrial epithelial cells than in proliferative ones (Fig. 2E). Next, we verified the expression of *GPX4* in primary endometrial epithelial cells of PCOS was significantly decreased, while no significant difference in endometrial stromal cells (Fig. 2F and G). Western blot and immunohistochemistry also consistently confirmed this result (Fig. 2H and I). Consistently, the expression of 4-Hydroxynonenal (4-HNE), a key target of ferroptosis, was obviously enhanced in epithelial cells (Fig. 2J). Therefore, we speculated that GPX4 might be the critical gene contribute to ferroptosis and GSH metabolism of PCOS endometrial epithelial cells.

3.3. GPX4 deficiency increased the sensitivity to oxidative stress of endometrial epithelial cells

To gain further insights into GPX4 in PCOS endometrial epithelial cells, we silenced ishikawa cells using *GPX4* small interfering RNA to evaluate the effect of reduced (but not completely eliminated) GPX4 activity on cell function (Fig. 3A). Cell viability analysis exhibited that si*GPX4* ishikawa cells were more sensitive to the ferroptosis inducer erastin (Fig. 3B). FerroOrange staining exhibited higher levels of Fe^{2+} (Fig. 3C) and lipid peroxidation in si*GPX4* ishikawa cells (Fig. 3D and E). We also observed the occurrence of ferroptosis related phenotypes such as increased malondialdehyde (MDA) and lipid peroxidation levels, decreased cell proliferation in ishikawa cells treated with GPX4 specific chemical inhibitor FIN56 (Fig. S2). These results indicated that knocked down *GPX4* in endometrial epithelial cells could activate ferroptosis. As is well known, PCOS is characterized by high androgen levels. To better investigate whether there was a relationship between androgens and ferroptosis, we primarily conducted correlation analysis and found the gene expression of *GPX4* was significantly negatively correlated with total testosterone levels and androgen receptor (*AR*) expression, independent of age and BMI adjustments (Fig. 3F). Subsequently, DHT intervention in ishikawa cells reduced GPX4 expression in a dose-dependent manner (Fig. 3G) and cell viability (Fig. 3H). Moreover, si*GPX4* ishikawa cells exacerbated the increase in MDA levels after application of DHT (Fig. 3I). Therefore, high androgen levels may aggravate the ferroptosis induced by GPX4 deficiency in endometrial epithelial cells.

3.4. Metabolomics revealed abnormal GSH metabolism of proliferative endometrium in PCOS

GSH, an important substance composed of glycine, glutamic acid, and cysteine, plays a key role in antagonizing ferroptosis. Down-regulation of the GSH metabolism pathway was enriched in both the previous scRNA-seq and transcriptomics analyses. Thus, to comprehensively discern the metabolic alterations in the endometrium of PCOS patients, we firstly conducted untargeted metabolomics. The orthogonal partial least squares discriminant analysis (OPLS-DA) score plot demonstrated the obvious discrimination between the PCOS and non-PCOS patients (Fig. 4A). A total of 245 differential metabolites were determined under four collection methods (Fig. 4B). As shown in the functional enrichment analysis, these differential metabolites were primarily enriched in multiple amino acid-related pathways, including GSH metabolism (Fig. 4C). To further quantify the changes of metabolites between the two groups, we performed the targeted metabolomics analysis (Fig. 4D). The volcano plot showed that there were 7 significantly increased metabolites and 31 decreased metabolites (Fig. 4E). KEGG analysis of the down-regulated differential metabolites enriched in the GSH metabolism, arginine and proline metabolism, lysine degradation pathway, while alpha−Linolenic acid metabolism and biosynthesis of unsaturated fatty acids were upregulated (Fig. 4F). Among them, glycine and pyroglutamic were involved in GSH metabolism pathway (Fig. 4G). Consistently, GSH content was also significantly downregulated in untargeted metabolomics (Fig.4H). Combined with the differential genes in transcriptomics, we drew a schematic

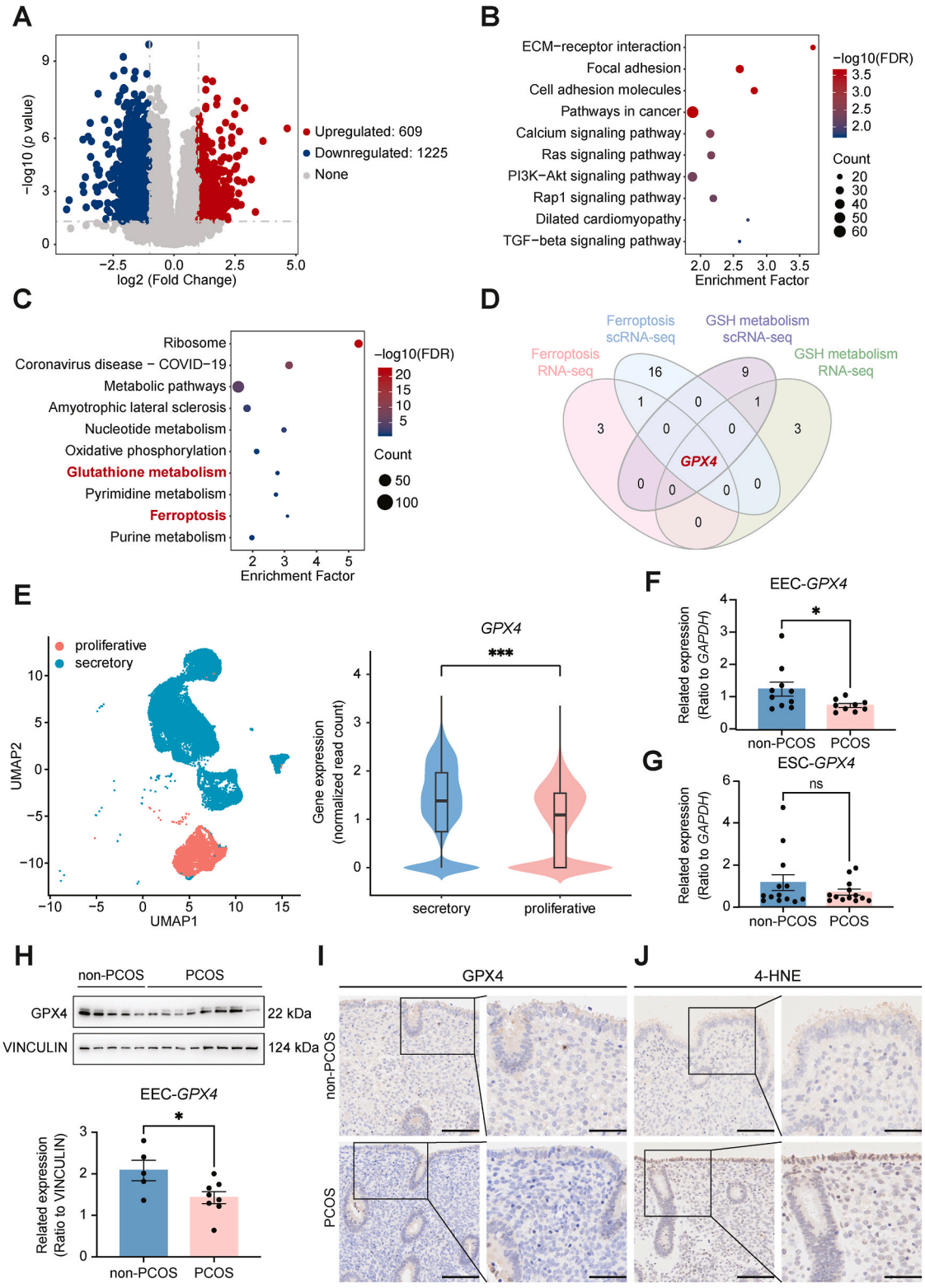

Fig. 2. The combined analysis of transcriptomics and scRNA-seq elucidated the key molecules and pathways influenced the endometrial dysfunction of PCOS. (**A**) Volcano plot of endometrial transcriptomics illustrated differentially expressed genes between PCOS and non-PCOS patients. Up-regulated genes were shown in red ($p < 0.05$); down-regulated genes were marked in blue ($p < 0.05$); non-significant genes were indicated in gray ($p > 0.05$). (**B** and **C**) KEGG pathway analysis of up-regulated (B) and down-regulated differential genes (C) in endometrium compared PCOS to non-PCOS patients. (**D**) Intersection of transcriptomics genes and scRNA-seq genes of ferroptosis pathway and GSH metabolism. (**E**) Distribution of *GPX4* in unciliated epithelium of the proliferative and secretory phases. (**F** and **G**) qPCR verified the expression of *GPX4* in endometrial epithelial cell (EEC) (F) and endometrial stromal cell (ESC) (G), respectively. (**H**) Western blot detected the expression of GPX4 in EEC. (**I** and **J**) Immunohistochemical staining of GPX4 (I) and 4-HNE (J) expression in endometrium from each group. Data are presented as mean ± SEM. Statistical analysis was performed using independent sample *t*-test or Mann-Whitney *U* test. $^{*}p < 0.05$, $^{**}p < 0.01$, $^{***}p < 0.001$.

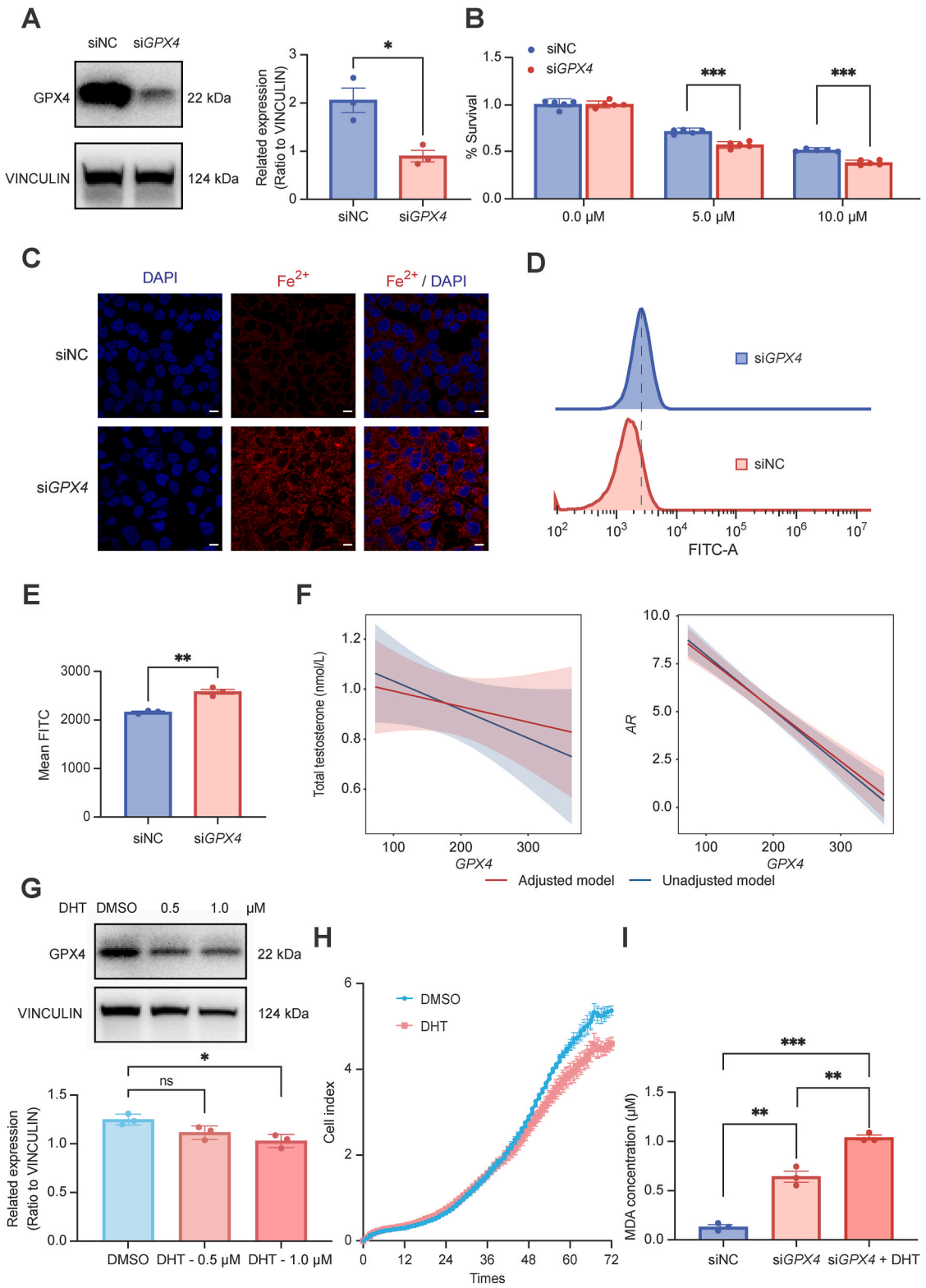

Fig. 3. GPX4 was a key molecule of ferroptosis in endometrial epithelial cells. (**A**) Left: The protein levels of GPX4 in si*GPX4* ishikawa cells detected by western blotting. Right: relative band intensities analyzed by ImageJ. (**B**) Cell viability of si*GPX4* and siNC ishikawa cells treated with erastin for 48 h measure by CCK8. (**C**) Intracellular Fe^{2+} level was detected by FerroOrange assay of si*GPX4* cells. Scale bar, 75 μm. (**D** and **E**) Flow cytometry analyzed ROS level of si*GPX4* cells. (**F**) Correlation analysis of the gene expression of *GPX4* with total testosterone levels and *AR* expression. Unadjusted model was shown in blue; adjusted model for age and BMI was shown in red. (**G**) Western blot detected the expression of GPX4 in ishikawa cells treated with different concentration of DHT. (**H**) Cell viability of ishikawa cells treated with DHT (1 μM). (**I**) MDA contents of si*GPX4* ishikawa cells treated with DHT for 48 h. Error bars, mean ± SEM. Statistical analysis was performed using independent sample *t*-test. $^{*}p < 0.05$, $^{**}p < 0.01$, $^{***}p < 0.001$.

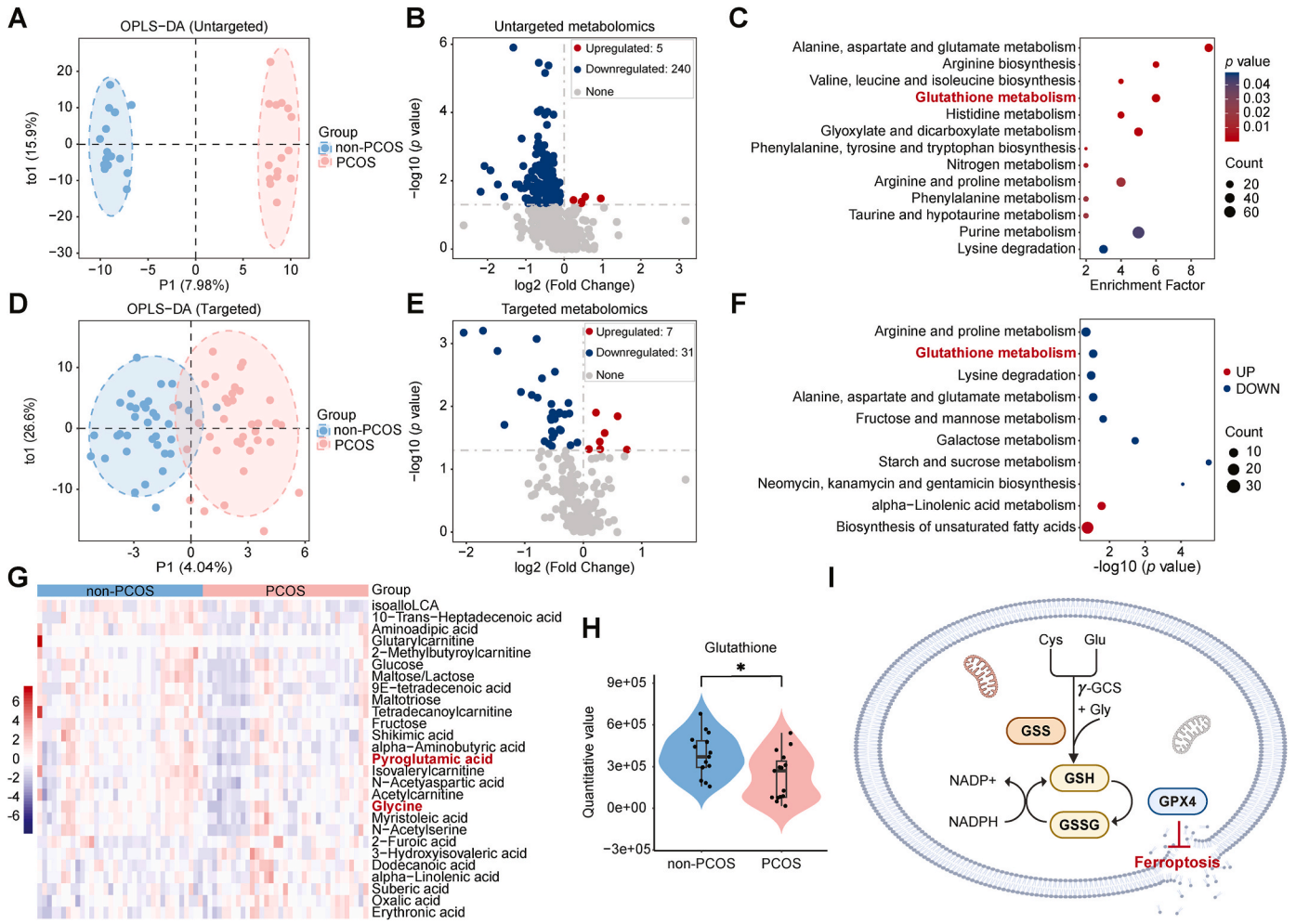

Fig. 4. Metabolomics revealed abnormal GSH metabolism of proliferative endometrium in PCOS. (**A** and **D**) OPLS-DA analysis of untargeted metabolomics (A) and targeted metabolomics (D) in the endometrium of PCOS and non-PCOS patients. Blue and red circles represent the non-PCOS and PCOS group, respectively. (**B** and **E**) Volcano plot of untargeted metabolomics (B) and targeted metabolomics (E) illustrated differential metabolites between PCOS and non-PCOS patients. (**C** and **F**) KEGG pathway analysis of untargeted metabolomics (C) and targeted metabolomics (F) of differential metabolites in endometrium compared PCOS to non-PCOS patients. (**G**) Heatmap shown the levels of top 20 differential metabolites from each sample of PCOS and non-PCOS patients. (**H**) GSH content in untargeted metabolomics. (**I**) A schematic diagram of GSH metabolism and ferroptosis. Cys: cysteine; Glu: glutamic acid; γ-GCS: γ-glutamylcysteine; Gly: glycine; GSS: glutathione synthetase; GSH: glutathione; GSSG: oxidized glutathione. Created with BioRender.com (https://biorender.com/).

diagram of GSH metabolism and the downstream ferroptosis changes in the proliferative endometrium of PCOS (Fig. 4I). Therefore, we speculated that the GSH depletion was an important factor for ferroptosis of PCOS endometrium.

3.5. *GPX4 deficiency contribute to fibrosis of epithelial cells though TGF-β1/Smad2/3 pathway*

Fibrosis is a primarily pathological outcome of ferroptosis induced by ECM remodeling in liver, kidney, heart, and other tissues [21]. To further discern possible downstream cell signaling pathways and biological processes regulated by ferroptosis, gene set variation analysis (GSVA) score partial correlation analysis was conducted using transcriptomics data. Ferroptosis was closely associated with fibrosis-related pathways, such as ECM-receptor interaction, focal adhesion, TGF-β signaling, as well as MAPK signaling pathway (Fig. 5A and Table S4). Moreover, the ECM-receptor interaction signaling pathway downregulated during the transition from the proliferative to the secretory phase of endometrial epithelial cells in previous analysis (Fig. 1E). These results suggested that excessive activation of ECM remodeling may be involved in dysfunction of endometrial epithelial cells in PCOS. Then, we focused on the changes in fibrosis mediated by GPX4 deficiency in epithelial cells. Masson staining shown the increased level of fibrosis in PCOS proliferative endometrium (Fig. 5B and C). Similar manifestations were presented in the uterus of DHT induced PCOS mice (Fig. 5D and E). We next investigated whether *GPX4* knockdown affected the expression of ECM-related genes. The mRNA expression of heparan-sulfate proteoglycan 2 (*HSPG2*), integrin beta 4 (*ITGB4*), integrin subunit alpha 9 (*ITGA9*), and bone morphogenetic protein 6 (*BMP6*) were increased in si*GPX4* ishikawa cells, which were differential genes enriched in the ECM-receptor interaction pathway in the transcriptomics (Fig. 5F). While there was no significant change of *COL4A2*, *THBS1*, *TNXB* and *LAMA5* in si*GPX4* ishikawa cells (Fig. S3). To deeper verify the potential mechanisms of fibrosis, we conducted GSEA enrichment analysis and found that the TGF–β1 signaling pathway was significantly upregulated in PCOS (Fig. 5G). TGF-β1 is the master factor that drives fibrosis through Smad-based and non-Smad-based signaling pathway [22]. The mRNA expression of transforming growth factor-β (*TGFB1*) was increased in si*GPX4* ishikawa cells (Fig. 5H). Besides, the protein expression of fibronectin and p-Smad2/3 significantly increased in si*GPX4* ishikawa cells (Fig. 5I). TGF-β1 treatment further exacerbated the upregulation of p-Smad2/3 protein expression in si*GPX4* ishikawa cells (Fig. 5I). Therefore, GPX4 deficiency may trigger fibrosis of PCOS endometrial epithelial cells through the TGF-β1/Smad2/3 pathway.

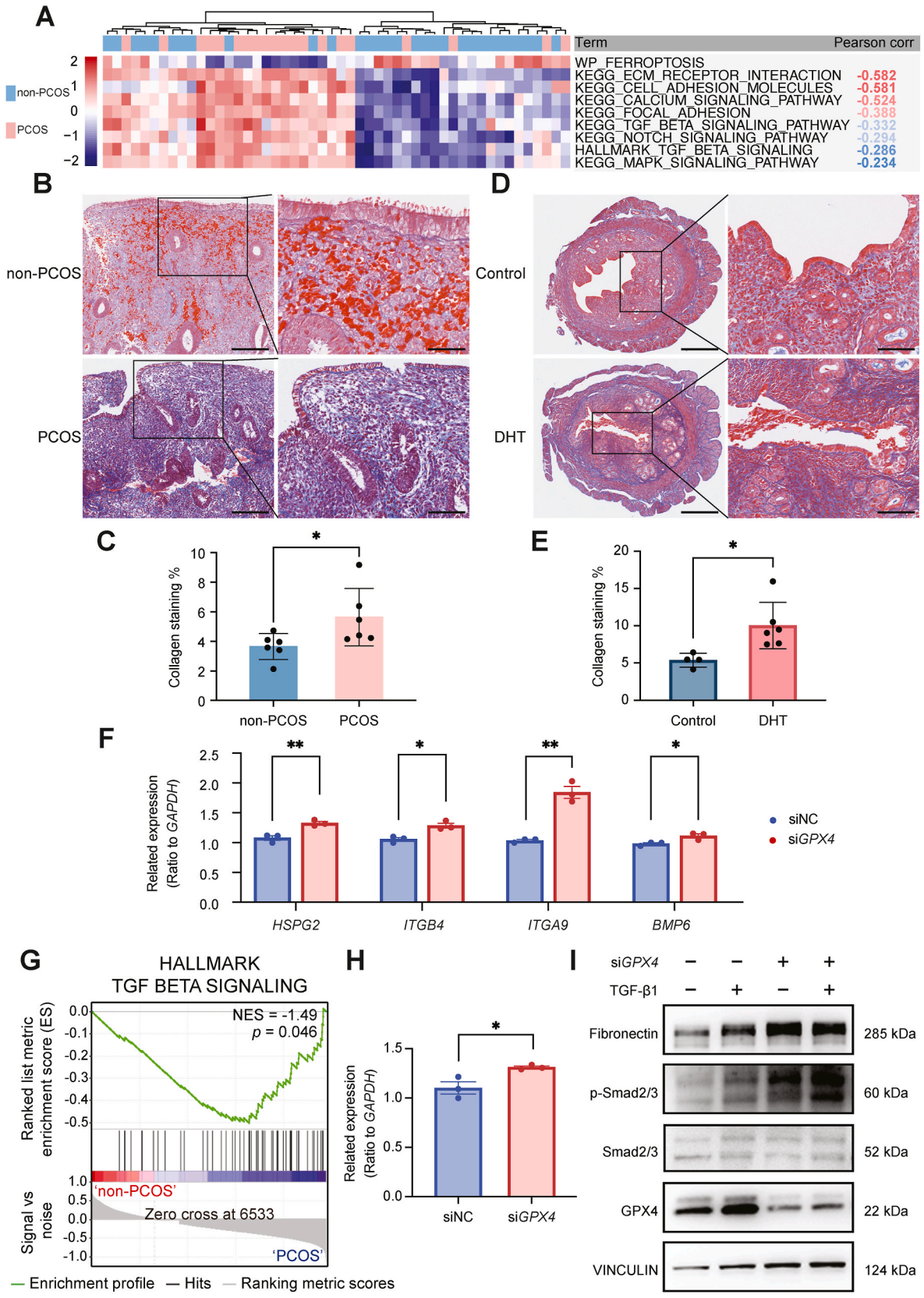

Fig. 5. GPX4 deficiency contribute to fibrosis of endometrial epithelial cells. (**A**) GSVA score of distinct biological processes and GSVA score partial correlation in non-PCOS and PCOS groups. (**B** and **D**) Masson trichrome staining images of non-PCOS and PCOS endometrium (B) and control and DHT uteri (D). Scale bar, 250 μm (left) and 50 (right) μm. (**C** and **E**) Quantitative statistical graph of Masson trichrome staining scores in two groups. (**F**) The mRNA expression of ECM-related genes of si*GPX4* ishikawa cells using qPCR. (**G**) GSEA enrichment analysis of TGF beta pathway in endometrium. (**H**) The mRNA expression of *TGFB1* of si*GPX4* ishikawa cells using qPCR. (**I**) Western blotting detected the phosphorylation level of Smad2/3 in si*GPX4* ishikawa cells treated with TGF-β1. Data are presented as mean ± SEM. Statistical analysis was performed using independent sample *t*-test. $^{*}p < 0.05$, $^{**}p < 0.01$, $^{***}p < 0.001$.

3.6. Inhibition of GPX4 caused the fibrotic phenotype of endometrial epithelial organoids

Endometrial organoids not only reproduce the structural and functional characteristics of the source tissue under in vitro hormone stimulation but also mimic the menstrual cycle, providing an ideal tool for studying human endometrial physiology and pathology. Therefore, to better elucidate the changes in ferroptosis and fibrosis during the periodic transition of PCOS endometrial epithelial cells, we collected endometrial tissues from PCOS and non-PCOS patients and isolated epithelial cells. Following the previously described method [23], we induced the formation of proliferative (Prol), secretory (Sec) and middle-secretory (Mid-sec) EEOs (Fig. 6A). From the 2-day culture period, EEOs gradually formed spheroid structures, and increased the number and diameter (Fig. 6B). The stromal cells obvious substantial declined during passage. EEOs became more mature and stable, and exhibited 3D configuration (Fig. 6B). To further decipher if ferroptosis in different phase of endometrium induced fibrosis, the GPX4 inhibitor FIN56 was employed. The GPX4 expression was obvious decreased in the four phases detected by western blotting and IF (Fig. 6C and Fig. S4). Moreover, compared to untreated non-PCOS patient (donor 1), the protein expression of fibrosis markers fibronectin was significantly increased in EEOs from basal to middle secretory phase (Fig. 6C–D and Fig. S5A). The elevated phosphorylation level of Smad2/3 was also observed in ExM and Prol phase (Fig. 6C–E and Fig. S5B). Hence, exposure to GPX4 deficiency could lead to the occurrence of fibrosis, which was caused by activation of Smad2/3 phosphorylation in proliferative EEOs.

3.7. Supplementing GSH improved the fibrotic phenotype of endometrial epithelial organoids

To further explore effective ways to ameliorate fibrosis, we treated EEOs with ferroptosis inhibitor GSH. To determine the optimal therapeutic concentration of GSH, we firstly treated EEOs of PCOS with different concentration gradients of GSH (0, 1, 10, 100 mM) for 48 h and detected the expression of fibrosis marker fibronectin (Fig. S6). Our results demonstrated that 1 mM and 10 mM GSH significantly reduced the expression of fibronectin in PCOS endometrial organoids compared with the non-PCOS endometrial organoids (Fig. S6). Notably, 100 mM GSH exhibited marked cytotoxicity, inducing substantial cell death (Fig. S6). Based on these findings, 1 mM GSH was selected as the optimal therapeutic concentration for subsequent experiments. We primarily detected strong expression of fibronectin in PCOS EEOs (donor 3) compared to non-PCOS patient (donor 2) at each stage (Fig. 7A and B and Figs. S5C–D). When treated GSH to PCOS EEOs, the expression of fibronectin was significant relieved (Fig. 7C and Fig. S5E). Therefore, supplementing GSH could improve the fibrotic phenotype of EEOs in PCOS. These findings collectively indicate that PCOS-specific declines in endometrial function, including GSH metabolism disorder, ferroptosis and fibrosis have already presented in endometrial epithelial cells. This may potentially impact the periodic changes of the endometrium and decidualization. The TGF-β1/Smad2/3 signaling pathway was activated in endometrial epithelial cells, which could give rise to overexpression of ECM-related genes (Fig. 7D).

4. Discussion

The lack of normal cyclic changes in the endometrium impaired the fertility of PCOS patients in childbearing age. Major findings from our study revealed the restriction of ferroptosis activity and ECM remodeling during the transition of the endometrium from the proliferative phase to the secretory phase in endometrial epithelial cells. Accordingly, ferroptosis due to GPX4 deficiency in PCOS proliferative endometrial epithelial cells might be the cause of periodic changes in their deficiency. High levels of androgens could exacerbate the degree of ferroptosis. Furthermore, the proliferative endometrium of PCOS had GSH metabolism disorders. Subsequently, using an endometrial EEOs model and cell lines in vitro, we revealed that inhibition of GPX4 could induce epithelial fibrosis through activation of TGF-β1/Smad2/3 pathway. Supplementing GSH could improve the fibrosis phenotype in EEOs. These findings contributed to elucidate the mechanism of PCOS endometrial dysfunction, which provided a new treatment strategy for improving clinical pregnancy outcomes and reducing the risk of endometrial lesions in PCOS patients.

Animal experiments found that continuous intraperitoneal injection of 5α-DHT and insulin into 7.5-day-old pregnant rats for one week resulted in ferroptosis. This phenomenon could be reversed by the antioxidant N-acetylcysteine (NAC) [24]. These findings were consistent with our research that DHT could inhibit the expression of GPX4 in endometrial epithelial cells. The potential role of androgens in ferroptosis has been elucidated in tumor cells. In prostate cancer cells, DHT strengthened the binding of *AR* to 2,4-Dienoyl-CoA Reductase 1 (*DECR1*) promoter regions, which in turn inhibited its transcription and then activated cell ferroptosis [25]. Controversially, AR was found to bind to *GPX4* promoter regions to promote its transcription in triple-negative breast cancer cell lines [26]. By reason of the foregoing, whether AR directly regulates the expression of GPX4 and then induces ferroptosis in epithelial cells in PCOS patients still needs more research to explore.

Ferroptosis was characterized by two hallmark features: iron accumulation and lipid peroxidation. The dynamic equilibrium of intracellular iron metabolism was coordinately regulated by transferrin receptor (TFRC) and the ferritin composed of ferritin light chain (FTL) and ferritin heavy chain (FTH) [27]. Extracellular Fe^{3+} was internalized into cells via TFRC-mediated endocytosis [27]. Our study revealed that the expression of *TFRC* and *FLT1* were significantly upregulated in EECs of PCOS, which may contribute to cellular iron overload (Figs. S6A and B). No significant difference was observed in *FTH1* mRNA expression (Fig. S6C). Previous studies have revealed a dual regulatory role of elevated FTL expression. On the one hand, it reduced intracellular free iron concentration through chelation, thereby attenuating Fenton reaction-driven ROS generation and lipid peroxide accumulation [28]. On the other hand, Elevated FTL expression, when accompanied by nuclear receptor coactivator 4 (NCOA4)-mediated enhancement of ferritin autophagy, might exacerbate ferroptosis through the release of iron storage. For instance, hypoxia-induced upregulation of FTL and downregulation of NCOA4 in macrophages suppressed ferritinophagy and consequently diminished cellular sensitivity to RSL3-induced ferroptosis [29]. Consistently, ferroptosis activation was accompanied by compensatory increases in FTH and FTL in the animal model of myocardial ischemic injury [30]. The precise alterations in endometrial iron metabolism and their downstream regulatory mechanisms in PCOS pathogenesis remain to be fully elucidated through further mechanistic studies.

Previous studies have not focused on the presence of collagen deposition and related tissue fibrosis in the endometrium of PCOS. Our study revealed the existence of this phenomenon for the first time. Combined with multi-omics data involving scRNA-seq, bulk transcriptomics and metabolomics analysis, the abnormal genes and metabolic profiles of PCOS endometrium were described. Then, from our experiment results and analysis, we confirmed that ferroptosis acts as a predisposing factor, triggering the fibrosis in endometrial epithelial cells of PCOS. As we know, fibrosis is manifested as excessive deposition of collagen, fibronectin, and proteoglycans in the ECM. Although fibrosis in the ovary of PCOS and mice have been clearly identified [31]. In addition, we observed a significant increase in the expression of connective tissue growth factor (*CTGF*), another fibrosis marker, in proliferative-phase endometrial epithelial cells of PCOS patients. CTGF, belongs to the CCN family, has been extensively reported as a pro-fibrotic mediator in multiple diseases such as liver fibrosis, pulmonary fibrosis, renal fibrosis, and cardiac fibrosis [32]. Mechanistically,

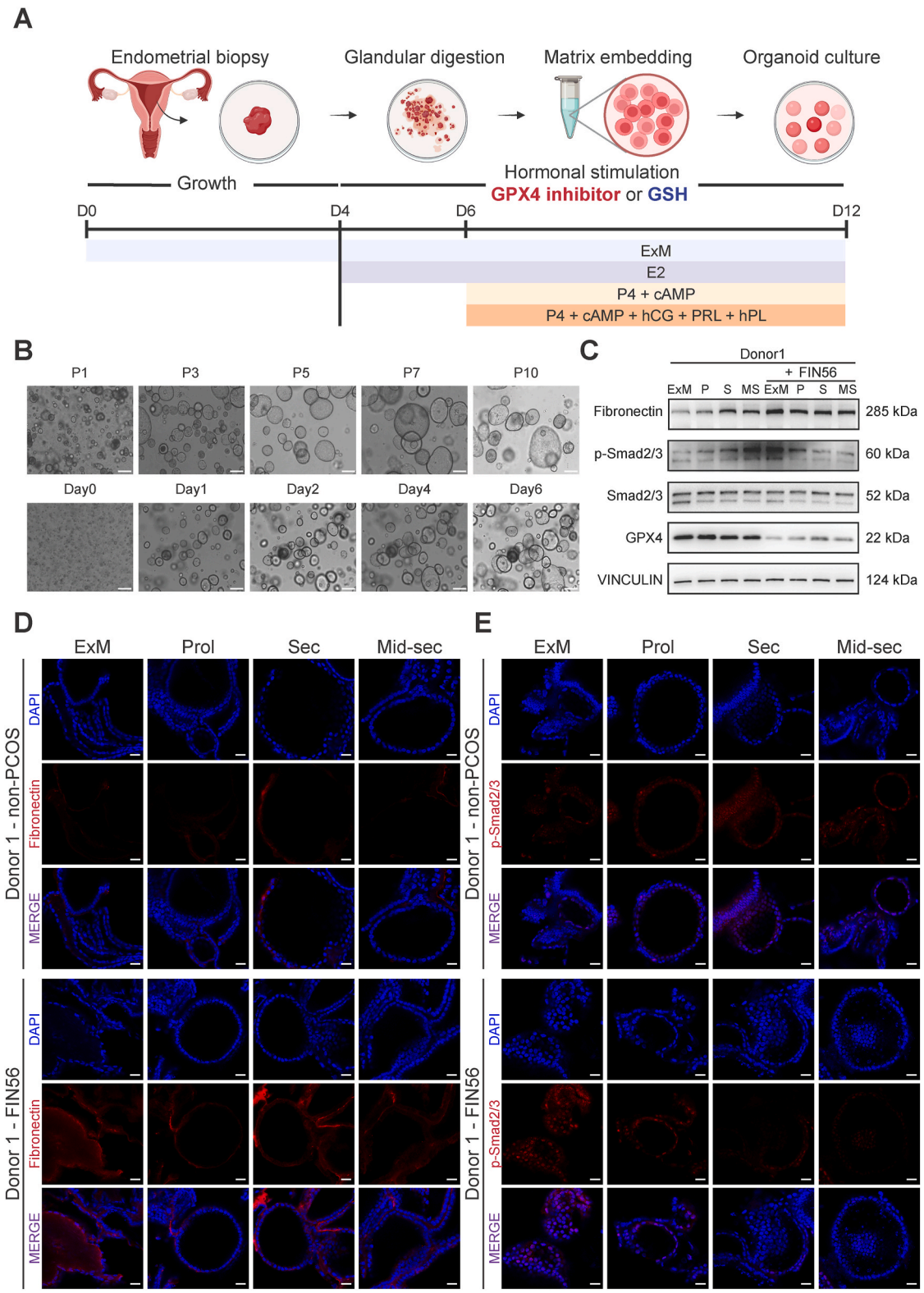

Fig. 6. GPX4 deficiency triggered the fibrotic phenotype of endometrial epithelial organoids. (**A**) Scheme for stimulation of endometrial organoids. Organoids were passaged and plated on day 0 (d0) in expansion medium (ExM). On d4, ExM was changed to different medium for 8 d. ExM: EEOs established in ExM continuously cultured. Prol: EEOs were primed with E2 to mimic proliferative endometrium. Sec: EEOs were primed with P4 + cAMP to mimic secretory endometrium. Mid-sec: EEOs were primed with differentiation medium (P4 + cAMP + hCG + PRL + hPL) to mimic endometrium during pregnancy. Created with BioRender.com (https://biorender.com/). (**B**) Typical bright field images of organoids with different generations (upper) and cultivation days (lower). (**C**) The protein expression of fibronectin, GPX4, Smad2/3 and phosphorylated Smad2/3 in EEOs from non-PCOS patient (donor 1) treated with or without FIN56. (**D**) IF staining of EEOs for fibronectin between non-PCOS patient (upper) and non-PCOS patient treated with FIN56 (lower). Scale bar, 20 μm. (**E**) IF staining of organoid for phosphorylated Smad2/3 between non-PCOS patient (upper) and non-PCOS patient treated with FIN56 (lower). Scale bar, 20 μm.

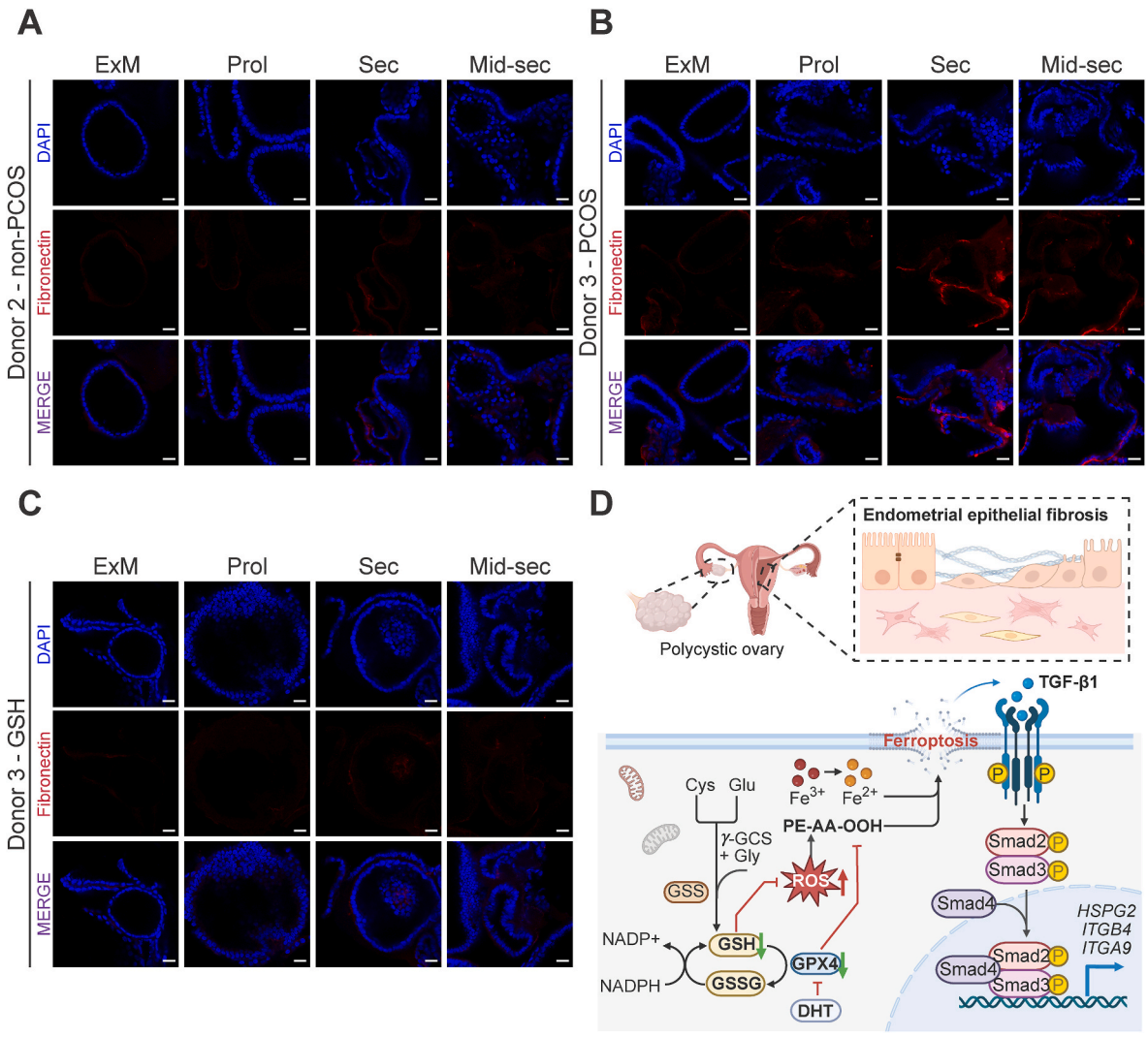

Fig. 7. Supplementing GSH rescued the fibrotic phenotype of endometrial epithelial organoids. (**A** and **B**) IF staining of organoids for fibronectin from non-PCOS (donor 2, A) and PCOS (donor 3, B) patient. Scale bar, 20 μm. (**C**) IF staining of organoids for fibronectin from PCOS (donor 3) patient treated with GSH. Scale bar, 20 μm. (**D**) Schematic diagram depicting proposed mechanism that ferroptosis induced by GPX4 deficiency, promoted endometrial epithelial fibrosis via the TGF-β1/Smad2/3 pathway. Cys: cysteine; Glu: glutamic acid; γ-GCS: γ-glutamylcysteine; Gly: glycine; GSS: glutathione synthetase; GSH: glutathione; GSSG: oxidized glutathione. Created with BioRender.com (https://biorender.com/).

TGF-β1 could enhance the expression of CTGF by activating the Smad2/3 signaling pathway, thereby driving fibrotic effect on lung epithelial cells and fibroblasts [33], hepatic stellate cells [34], and proximal-tubule epithelial cells [35]. Therefore, we speculate that the activation of the TGF-β1/Smad2/3 pathway in proliferative endometrial epithelial cells of PCOS may also promote fibrosis by promoting the expression of CTGF. However, it is not yet clear whether there was a fibrotic phenotype would lead to the loss of cyclical transformation in the endometrium of PCOS.

In addition, our study suggests that knocking down *GPX4* in endometrial epithelial cells leads to increased expression of multiple downstream genes by activating Smad2/3 phosphorylation. HSPG2 is a heparan sulfate proteoglycan that typically exists at the boundary between epithelial and connective tissues. Our study provided an insight into how knocked down *GPX4* in endometrial epithelial cells contributed to increase the expression of multiple downstream genes by activating Smad2/3 phosphorylation. Among them, HSPG2 encoded a heparan sulfate proteoglycan that typically existed at the boundary between epithelial and connective tissues. It was been reported to have Smad3 binding sites in the promoter region [36] and synergistically activated fibrosis of hypertrophic scar fibroblast with TNFSF13 [37]. Besides, ITGB4 could promote the phosphorylation of Smad1/5 and ubiquitination of Smad4 though MAPK-ERK axis, which mediated the endothelial-to-mesenchymal transition [38]. ITGA9, a major ECM protein, have also been reported to be significantly upregulated in renal fibrosis [39]. Moreover, utilizing published Smad2/3 ChIP-seq data in the human breast cancer cell line BT-549 (GSE104352), human immortalized keratinocytes (HaCaT, GSE189303), and human primary epidermal keratinocytes (HPEK, GSE180252) stimulated with TGF-β, we observed Smad2 and/or Smad3 binding in the regulatory regions of HSPG2 and ITGB4 as well as other fibrosis-related genes (Fig. S8). These observations partially confirm that Smad2/3 can regulate HSPG2 and ITGB4 directly, although behaviors of transcription factors are tissue- or even cell-type-specific. Future Smad2/3 ChIP-seq data in human endometrial epithelial cells will further clarify the regulatory relationship between Smad2/3 and downstream genes.

In order to better simulate the status of PCOS endometrial epithelial cells in different cycles, we established a PCOS organoid model that was more closely to real physiological environment for molecular mechanism verification. During our experiment, we were surprised to find that GPX4 deficiency induced the elevated level of fibronectin protein expression through non Smad2/3 pathways during the secretory and

mid-secretory phase. However, the limitation of our study was not yet evaluated the pathogenic mechanism of this phenomenon in endometrial samples of secretory PCOS patients, and more experiments are needed to explore it in the future.

In addition, previous research has found that a Ru-Single-Atom Nanozyme (Ru-SAN) incorporated into chitosan hydrogel could enhance endometrial regeneration to treat intrauterine adhesion, a disease characterized by excessive fibrosis and impaired reproductive function [40]. Ru-SAN targeted ferroptosis to restore the structure and thickness of uterine glands [40]. Similarly, a sprayable hydrogel designed a collagen-binding peptide with glutathione, combined with human endometrial organoid extracellular vesicles (HEO-EVs), could promote angiogenesis and prevent endometrial fibrosis, thus effectively enhanced the fertility of mouse models with endometrial damage [41]. The clinical application of GSH has accumulated evidence-based evidence in nonalcoholic fatty liver disease (300 mg/day, oral treatment for 4 months) [42], chronic hepatitis B (1.2 g reduced GSH, intravenous infusion, 1 day/times for 3 months) [43], acute kidney injury caused by cisplatin (intravenous infusion) [44], Parkinson's disease (100 mg or 200 mg GSH, intranasal administration, thrice daily for three months) [45], type 2 diabetes (oral liposome GSH, 1260 mg/day for three months) [46]. Notably, the sublingual form of GSH demonstrated superior bioavailability compared to oral NAC and GSH formulations by allowing to by-pass the effect of hepatic first-pass metabolism and enzymatic degradation in the intestine [47]. Although direct clinical evidence for GSH in endometrial disorders remains limited, optimized delivery strategies provide insights into its potential application for endometrial dysfunction in PCOS. Importantly, NAC, a biosynthetic precursor of GSH, has shown clinical value in endometriosis management. Two prospective cohort studies revealed that oral NAC treatment (600 mg/dose, thrice daily for 3 consecutive days weekly) significantly reduced endometriotic cyst size and pain severity in patients, with superior outcomes compared to hormonal therapy and improved fertility in patients [48]. These findings suggest that oral GSH supplementation may represent a potential intervention strategy for ameliorating endometrial microenvironment abnormalities in PCOS, warranting further clinical studies to validate its efficacy and safety.

5. Conclusion

In conclusion, the study demonstrated important functional alterations in PCOS endometrium, including ferroptosis and fibrosis. The effects of changes in a variety of molecules and metabolites were observed and validated using endometrium tissues, cell lines and organoids. Our work was the first to identify a strong correlation with the GPX4 - TGF-β1/Smad2/3 signaling pathway and fibrosis in PCOS endometrial epithelial cells. These findings may consider as a promising strategy in the therapeutics of improving endometrial function in PCOS.

The data are available upon reasonable request. All relevant data were included in this published article and its supplementary information files.

CRediT authorship contribution statement

Zhenhong Ye: Writing – review & editing, Writing – original draft, Software, Methodology, Investigation, Funding acquisition, Data curation. **Ming Cheng:** Writing – review & editing, Visualization, Software, Methodology. **Weisi Lian:** Writing – original draft, Validation, Methodology, Investigation. **Yueqi Leng:** Methodology, Investigation. **Xunsi Qin:** Methodology. **Yue Wang:** Methodology. **Ping Zhou:** Methodology. **Xiyao Liu:** Visualization, Software. **Tianliu Peng:** Methodology. **Ruiqi Wang:** Investigation. **Yilei He:** Funding acquisition. **Heng Pan:** Writing – review & editing, Validation. **Yue Zhao:** Writing – review & editing, Validation, Supervision, Project administration. **Rong Li:** Validation, Supervision, Project administration, Funding acquisition, Conceptualization.

Declaration of competing interest

The authors declare no conflict of interest.

Acknowledgements

We express our gratitude to the all the sample donors and the doctors and nurses of the Reproductive Medical Center of Peking University Third Hospital for their excellent assistance. We thank for the numerous researchers who contributed to the collection, phenotypic characterization of clinical samples, and the analysis and public availability of data. This study was supported by the National Key Research and Development Project of China (2022YFC2702500), the National Natural Science Foundation of China (81925013, 82288102, 823B2032, 82301842, 82271699), the Key Projects of Yunnan Province Science and Technology Department (202302AA310044), the Frontiers Medical Center, Tianfu Jincheng Laboratory Foundation (TFJC2023010001), the Key Clinical Projects of Peking University Third Hospital (BYSY2022043, BYSYZD2023028), the Beijing Nova Program (20220484073). None of the funding sources in this study played a role in the study design, data collection, data analysis, interpretation, or manuscript writing.

Appendix A. Supplementary data

Supplementary data to this article can be found online at https://doi.org/10.1016/j.redox.2025.103615.

Data availability

Data will be made available on request.

References

[1] R. Yang, Q. Li, Z. Zhou, W. Qian, J. Zhang, Z. Wu, L. Jin, X. Wu, C. Zhang, B. Zheng, J. Tan, G. Hao, S. Li, T. Tian, Y. Hao, D. Zheng, Y. Wang, R.J. Norman, R. Li, P. Liu, J. Qiao, Lancet Reg Health West Pac 25 (2022) 100494, https://doi.org/10.1016/j.lanwpc.2022.100494.
[2] H.F. Escobar-Morreale, Nat. Rev. Endocrinol. 14 (5) (2018) 270, https://doi.org/10.1038/nrendo.2018.24.
[3] M.O. Goodarzi, D.A. Dumesic, G. Chazenbalk, R. Azziz, Nat. Rev. Endocrinol. 7 (4) (2011) 219, https://doi.org/10.1038/nrendo.2010.217.
[4] S. Palomba, M.A. de Wilde, A. Falbo, M.P. Koster, G.B. La Sala, B.C. Fauser, Hum. Reprod. Update 21 (5) (2015) 575, https://doi.org/10.1093/humupd/dmv029.
[5] S. Liu, M. Mo, S. Xiao, L. Li, X. Hu, L. Hong, L. Wang, R. Lian, C. Huang, Y. Zeng, L. Diao, Front. Endocrinol. 11 (2020) 575337, https://doi.org/10.3389/fendo.2020.575337.
[6] J. Cha, X. Sun, S.K. Dey, Nat. Med. 18 (12) (2012) 1754, https://doi.org/10.1038/nm.3012.
[7] L.A. Salamonsen, J.C. Hutchison, C.E. Gargett, Development 148 (17) (2021), https://doi.org/10.1242/dev.199577.
[8] E. Stener-Victorin, H. Teede, R.J. Norman, R. Legro, M.O. Goodarzi, A. Dokras, J. Laven, K. Hoeger, T.T. Piltonen, Nat. Rev. Dis. Primers 10 (1) (2024) 27, https://doi.org/10.1038/s41572-024-00511-3.
[9] X. Li, Y. Lin, X. Cheng, G. Yao, J. Yao, S. Hu, Q. Zhu, Y. Wang, Y. Ding, Y. Lu, J. Qi, H. Zhao, X. Bian, Y. Du, K. Sun, H. Vankelecom, Y. Sun, Hum Reprod Open 2024 (2) (2024) hoae013, https://doi.org/10.1093/hropen/hoae013.
[10] Y. Lu, Y. Shao, W. Cui, Z. Jia, Q. Zhang, Q. Zhao, Z.J. Chen, J. Yan, B. Chu, J. Yuan, Adv. Sci. 11 (4) (2024) e2302887, https://doi.org/10.1002/advs.202302887.
[11] G. Li, Y. Lin, Y. Zhang, N. Gu, B. Yang, S. Shan, N. Liu, J. Ouyang, Y. Yang, F. Sun, H. Xu, Cell Death Dis. 8 (1) (2022) 29, https://doi.org/10.1038/s41420-022-00821-z.
[12] M. Murri, M. Luque-Ramírez, M. Insenser, M. Ojeda-Ojeda, H.F. Escobar-Morreale, Hum. Reprod. Update 19 (3) (2013) 268, https://doi.org/10.1093/humupd/dms059.
[13] B.R. Stockwell, J.P. Friedmann Angeli, H. Bayir, A.I. Bush, M. Conrad, S.J. Dixon, S. Fulda, S. Gascón, S.K. Hatzios, V.E. Kagan, K. Noel, X. Jiang, A. Linkermann, M. E. Murphy, M. Overholtzer, A. Oyagi, G.C. Pagnussat, J. Park, Q. Ran, C. S. Rosenfeld, K. Salnikow, D. Tang, F.M. Torti, S.V. Torti, S. Toyokuni, K. A. Woerpel, D.D. Zhang, Cell 171 (2) (2017) 273, https://doi.org/10.1016/j.cell.2017.09.021.
[14] X. Jiang, B.R. Stockwell, M. Conrad, Nat. Rev. Mol. Cell Biol. 22 (4) (2021) 266, https://doi.org/10.1038/s41580-020-00324-8.
[15] D. Tang, X. Chen, R. Kang, G. Kroemer, Cell Res. 31 (2) (2021) 107, https://doi.org/10.1038/s41422-020-00441-1.

[16] S. Aibar, C.B. González-Blas, T. Moerman, V.A. Huynh-Thu, H. Imrichova, G. Hulselmans, F. Rambow, J.C. Marine, P. Geurts, J. Aerts, J. van den Oord, Z. K. Atak, J. Wouters, S. Aerts, Nat. Methods 14 (11) (2017) 1083, https://doi.org/10.1038/nmeth.4463.

[17] C. Wang, L. Wang, Q. Zhao, J. Ma, Y. Li, J. Kuang, X. Yang, H. Bi, A. Lu, K.C. P. Cheung, G. Melino, W. Jia, Cell Death Differ. 31 (12) (2024) 1625, https://doi.org/10.1038/s41418-024-01394-3.

[18] Y. Zhang, Z. Yan, Q. Qin, V. Nisenblat, H.M. Chang, Y. Yu, T. Wang, C. Lu, M. Yang, S. Yang, Y. Yao, X. Zhu, X. Xia, Y. Dang, Y. Ren, P. Yuan, R. Li, P. Liu, H. Guo, J. Han, H. He, K. Zhang, Y. Wang, Y. Wu, M. Li, J. Qiao, J. Yan, L. Yan, Mol. Cell 72 (6) (2018) 1021, https://doi.org/10.1016/j.molcel.2018.10.029.

[19] T. Peng, S. Yang, W. Lian, X. Liu, P. Zheng, X. Qin, B. Liao, P. Zhou, Y. Wang, F. Liu, Z. Yang, Z. Ye, H. Shan, X. Liu, Y. Yu, R. Li, Hum. Reprod. 39 (8) (2024) 1778, https://doi.org/10.1093/humrep/deae137.

[20] W. Wang, F. Vilella, P. Alama, I. Moreno, M. Mignardi, A. Isakova, W. Pan, C. Simon, S.R. Quake, Nat. Med. 26 (10) (2020) 1644, https://doi.org/10.1038/s41591-020-1040-z.

[21] a) P. Horn, F. Tacke, Cell Metab. 36 (7) (2024) 1439, https://doi.org/10.1016/j.cmet.2024.05.003;
b) Q. Feng, Y. Yang, K. Ren, Y. Qiao, Z. Sun, S. Pan, F. Liu, Y. Liu, J. Huo, D. Liu, Z. Liu, Int. J. Biol. Sci. 19 (12) (2023) 3726, https://doi.org/10.7150/ijbs.85674;
c) Y. Chen, X. Li, S. Wang, R. Miao, J. Zhong, Nutrients 15 (3) (2023), https://doi.org/10.3390/nu15030591.

[22] X.M. Meng, D.J. Nikolic-Paterson, H.Y. Lan, Nat. Rev. Nephrol. 12 (6) (2016) 325, https://doi.org/10.1038/nrneph.2016.48.

[23] M.Y. Turco, L. Gardner, J. Hughes, T. Cindrova-Davies, M.J. Gomez, L. Farrell, M. Hollinshead, S.G.E. Marsh, J.J. Brosens, H.O. Critchley, B.D. Simons, M. Hemberger, B.K. Koo, A. Moffett, G.J. Burton, Nat. Cell Biol. 19 (5) (2017) 568, https://doi.org/10.1038/ncb3516.

[24] a) Y. Zhang, M. Hu, W. Jia, G. Liu, J. Zhang, B. Wang, J. Li, P. Cui, X. Li, S. Lager, A.N. Sferruzzi-Perri, Y. Han, S. Liu, X. Wu, M. Brännström, L.R. Shao, H. Billig, J. Endocrinol. 246 (3) (2020) 247, https://doi.org/10.1530/joe-20-0155;
b) M. Hu, Y. Zhang, S. Ma, J. Li, X. Wang, M. Liang, A.N. Sferruzzi-Perri, X. Wu, H. Ma, M. Brännström, L.R. Shao, H. Billig, Mol. Hum. Reprod. 27 (12) (2021), https://doi.org/10.1093/molehr/gaab067.

[25] Z.D. Nassar, C.Y. Mah, J. Dehairs, I.J. Burvenich, S. Irani, M.M. Centenera, M. Helm, R.K. Shrestha, M. Moldovan, A.S. Don, J. Holst, A.M. Scott, L.G. Horvath, D.J. Lynn, L.A. Selth, A.J. Hoy, J.V. Swinnen, L.M. Butler, Elife 9 (2020), https://doi.org/10.7554/eLife.54166.

[26] F. Yang, Y. Xiao, J.H. Ding, X. Jin, D. Ma, D.Q. Li, J.X. Shi, W. Huang, Y.P. Wang, Y. Z. Jiang, Z.M. Shao, Cell Metab. 35 (1) (2023) 84, https://doi.org/10.1016/j.cmet.2022.09.021.

[27] S. Dutt, I. Hamza, T.B. Bartnikas, Annu. Rev. Nutr. 42 (2022) 311, https://doi.org/10.1146/annurev-nutr-062320-112625.

[28] Q. Ru, Y. Li, L. Chen, Y. Wu, J. Min, F. Wang, Signal Transduct. Targeted Ther. 9 (1) (2024) 271, https://doi.org/10.1038/s41392-024-01969-z.

[29] D.C. Fuhrmann, A. Mondorf, J. Beifuß, M. Jung, B. Brüne, Redox Biol. 36 (2020) 101670, https://doi.org/10.1016/j.redox.2020.101670.

[30] X. Fang, H. Wang, D. Han, E. Xie, X. Yang, J. Wei, S. Gu, F. Gao, N. Zhu, X. Yin, Q. Cheng, P. Zhang, W. Dai, J. Chen, F. Yang, H.T. Yang, A. Linkermann, W. Gu, J. Min, F. Wang, Proc. Natl. Acad. Sci. U. S. A. 116 (7) (2019) 2672, https://doi.org/10.1073/pnas.1821022116.

[31] a) D. Wang, Y. Weng, Y. Zhang, R. Wang, T. Wang, J. Zhou, S. Shen, H. Wang, Y. Wang, Sci. Total Environ. 745 (2020) 141049, https://doi.org/10.1016/j.scitotenv.2020.141049;
b) N. Takahashi, M. Harada, Y. Hirota, E. Nose, J.M. Azhary, H. Koike, C. Kunitomi, O. Yoshino, G. Izumi, T. Hirata, K. Koga, O. Wada-Hiraike, R. J. Chang, S. Shimasaki, T. Fujii, Y. Osuga, Sci. Rep. 7 (1) (2017) 10824, https://doi.org/10.1038/s41598-017-11252-7.

[32] M. Fu, D. Peng, T. Lan, Y. Wei, X. Wei, Acta Pharm. Sin. B 12 (4) (2022) 1740, https://doi.org/10.1016/j.apsb.2022.01.007.

[33] a) Q. Ding, I. Subramanian, T.R. Luckhardt, P. Che, M. Waghray, X.K. Zhao, N. Bone, A.R. Kurundkar, L. Hecker, M. Hu, Y. Zhou, J.C. Horowitz, R. Vittal, V. J. Thannickal, Am. J. Physiol. Lung Cell. Mol. Physiol. 312 (6) (2017) L926, https://doi.org/10.1152/ajplung.00121.2016;
b) X. Sun, X. Cui, X. Chen, X. Jiang, Biomed. Pharmacother. 131 (2020) 110744, https://doi.org/10.1016/j.biopha.2020.110744.

[34] E. Hernández-Aquino, M.A. Quezada-Ramírez, A. Silva-Olivares, S. Casas-Grajales, E. Ramos-Tovar, R.E. Flores-Beltrán, J. Segovia, M. Shibayama, P. Muriel, Eur. J. Pharmacol. 865 (2019) 172730, https://doi.org/10.1016/j.ejphar.2019.172730.

[35] M.K. Phanish, N.A. Wahab, P. Colville-Nash, B.M. Hendry, M.E. Dockrell, Biochem. J. 393 (Pt 2) (2006) 601, https://doi.org/10.1042/bj20051106.

[36] C.R. Warren, B.J. Grindel, L. Francis, D.D. Carson, M.C. Farach-Carson, J. Cell. Biochem. 115 (7) (2014) 1322, https://doi.org/10.1002/jcb.24788.

[37] H. Zhang, C. Zang, W. Zhao, L. Zhang, R. Liu, Z. Feng, J. Wu, R. Cui, Int. J. Nanomed. 18 (2023) 7047, https://doi.org/10.2147/ijn.S433510.

[38] Q. He, J. Li, C. Tao, C. Zeng, C. Liu, Z. Zheng, S. Mou, W. Liu, B. Zhang, X. Yu, Y. Zhai, J. Wang, Q. Zhang, Y. Zhang, D. Zhang, J. Zhao, P. Ge, MedComm 5 (5) (2020) e525, https://doi.org/10.1002/mco2.525, 2024.

[39] S. Jin, Y. Song, L. Zhou, W. Jiang, L. Qin, Y. Wang, R. Yu, Y. Liu, Y. Diao, F. Zhang, K. Liu, P. Li, H. Hu, B. Jiang, W. Tang, F. Yi, Y. Gong, G. Liu, G. Sun, Cell Rep. 42 (6) (2023) 112550, https://doi.org/10.1016/j.celrep.2023.112550.

[40] Y. Liang, J. Meng, Z. Yu, Y. Guo, X. Zhang, Y. Yan, S. Du, S. Jin, J. Li, H. Yang, X. Zhang, Z. Liu, L. Li, J. Xie, Biomaterials 315 (2025) 122923, https://doi.org/10.1016/j.biomaterials.2024.122923.

[41] X. Qin, K.L. Hu, Q. Li, Y. Sun, T. Peng, X. Liu, J. Li, W. Nan, Y. Yu, X. Qi, R. Li, Adv. Healthcare Mater. (2024) e2403604, https://doi.org/10.1002/adhm.202403604.

[42] Y. Honda, T. Kessoku, Y. Sumida, T. Kobayashi, T. Kato, Y. Ogawa, W. Tomeno, K. Imajo, K. Fujita, M. Yoneda, K. Kataoka, M. Taguri, T. Yamanaka, Y. Seko, S. Tanaka, S. Saito, M. Ono, S. Oeda, Y. Eguchi, W. Aoi, K. Sato, Y. Itoh, A. Nakajima, BMC Gastroenterol. 17 (1) (2017) 96, https://doi.org/10.1186/s12876-017-0652-3.

[43] Q. Wei, J. Zhao, BMC Gastroenterol. 25 (1) (2025) 68, https://doi.org/10.1186/s12876-025-03600-z.

[44] Y. Huang, Y. Li, X. Xu, J. Teng, X. Ding, J. Xu, Ren. Fail. 46 (2) (2024) 2411359, https://doi.org/10.1080/0886022x.2024.2411359.

[45] L.K. Mischley, R.C. Lau, E.G. Shankland, T.K. Wilbur, J.M. Padowski, J. Parkinsons Dis. 7 (2) (2017) 289, https://doi.org/10.3233/jpd-161040.

[46] K. To, R. Cao, A. Yegiazaryan, J. Owens, T. Nguyen, K. Sasaninia, C. Vaughn, M. Singh, E. Truong, A. Medina, E. Avitia, J. Villegas, C. Pham, A. Sathananthan, V. Venketaraman, Front. Cell. Infect. Microbiol. 11 (2021) 657775, https://doi.org/10.3389/fcimb.2021.657775.

[47] B. Schmitt, M. Vicenzi, C. Garrel, F.M. Denis, Redox Biol. 6 (2015) 198, https://doi.org/10.1016/j.redox.2015.07.012.

[48] a) M.G. Porpora, R. Brunelli, G. Costa, L. Imperiale, E.K. Krasnowska, T. Lundeberg, I. Nofroni, M.G. Piccioni, E. Pittaluga, A. Ticino, T. Parasassi, Evid Based Complement Alternat Med 2013 (2013) 240702, https://doi.org/10.1155/2013/240702;
b) E. Anastasi, S. Scaramuzzino, M.F. Viscardi, V. Viggiani, M.G. Piccioni, L. Cacciamani, L. Merlino, A. Angeloni, L. Muzii, M.G. Porpora, Int. J. Environ. Res. Publ. Health 20 (6) (2023), https://doi.org/10.3390/ijerph20064686.